The Journal of Experimental Biology 208, 3771-3783
Published by The Company of Biologists 2005
doi:10.1242/jeb.01829

Sulphonylurea sensitivity and enriched expression implicate inward rectifier K^+ channels in *Drosophila melanogaster* renal function

Jennifer M. Evans, Adrian K. Allan, Shireen A. Davies and Julian A. T. Dow*

Division of Molecular Genetics, Faculty of Biomedical and Life Sciences, University of Glasgow, Glasgow, G11 6NU, UK

*Author for correspondence (e-mail: j.a.t.dow@bio.gla.ac.uk)

Accepted 10 August 2005

Summary

Insect Malpighian (renal) tubules are capable of transporting fluid at remarkable rates. Secondary active transport of potassium at the apical surface of the principal cell must be matched by a high-capacity basolateral potassium entry route. A recent microarray analysis of *Drosophila* tubule identified three extremely abundant and enriched K^+ channel genes encoding the three inward rectifier channels of *Drosophila*: *ir*, *irk2* and *irk3*. Enriched expression of inward rectifier channels in tubule was verified by quantitative RT-PCR, and all three IRKs localised to principal cells of the main segment (and *ir* and *irk3* to the lower tubule) by *in situ* hybridisation, suggesting roles both in primary secretion and reabsorption. A new splice form of *irk2* was also identified. The role of inward rectifiers in fluid secretion was assessed with a panel of selective inhibitors of inward rectifier channels, the antidiabetic sulphonylureas. All completely inhibited fluid secretion, with IC_{50}s of 0.78 mmol l^{-1} for glibenclamide and approximately 5 mmol l^{-1} for tolbutamide, 0.01 mmol l^{-1} for minoxidil and 0.1 mmol l^{-1} for diazoxide. This pharmacology is consistent with a lower-affinity class of inward rectifier channel that does not form an obligate multimer with the sulphonylurea receptor (SUR), although effects on non-IRK targets cannot be excluded. Glibenclamide inhibited fluid secretion similarly to basolateral K^+-free saline.

Radiolabelled glibenclamide is both potently transported and metabolised by tubule. Furthermore, glibenclamide is capable of blocking transport of the organic dye amaranth (azorubin S), at concentrations of glibenclamide much lower than required to impact on fluid secretion. Glibenclamide thus interacts with tubule in three separate ways; as a potent inhibitor of fluid secretion, as an inhibitor (possibly competitive) of an organic solute transporter and as a substrate for excretion and metabolism.

Key words: *ir*, *irk2*, *irk3*, glibenclamide, inward rectifier channel, Malpighian tubule, functional genomics, *Drosophila melanogaster*.

Introduction

Fluid-secreting epithelia must achieve high fluxes of cations, anions, water and other solutes. A striking exemplar of such transport is offered by the Malpighian (renal) tubules of insects, which, when maximally stimulated, are capable of transporting their own cell volumes of fluid every 10 s – rates unmatched elsewhere in biology (Dow and Davies, 2003; Maddrell, 1991). In insects, an apical plasma membrane V-ATPase energises a proton/alkali-metal cation exchanger, thought to prefer potassium over sodium (Wieczorek et al., 1999). Potassium enters the cell from the basolateral surface through a combination of a ouabain-sensitive Na^+/K^+-ATPase (Torrie et al., 2004), a $Na^+/K^+/2Cl^-$ cotransporter (Ianowski and O'Donnell, 2004) and barium-sensitive potassium channels (Beyenbach and Masia, 2002; Masia et al., 2000; Weltens et al., 1992); their relative importance may vary between insects. Present estimates suggest that, in *Drosophila*, each contributes approximately equally to the K^+ flux (Torrie et al., 2004). At a transepithelial level, therefore, potassium appears to be actively transported. The route for the passive anion shunt is controversial; but in *Drosophila*, it is regulated by stellate cells (Denholm et al., 2003; O'Donnell et al., 1996; Radford et al., 2002); there is evidence that these cells also contain aquaporins (Dow et al., 1995; Kaufmann et al., 2004), so providing a low-resistance shunt pathway for both anions and water.

Drosophila melanogaster, despite its small size, offers unique advantages for the study of epithelial physiology, and accordingly, the molecular basis of *D. melanogaster* renal function is now understood in considerable detail (Dow and Davies, 2001, 2003). Among the tools available to the *Drosophila* community is a comprehensive Affymetrix microarray, which allows gene expression to be studied quantitatively over space and time. A recent such study, comparing adult *Drosophila* tubule with whole flies, identified genes that are either abundantly expressed or highly enriched in tubule (Wang et al., 2004). Thus, this study both identifies

Table 1. *Primers used for qPCR*

Gene	Forward	Reverse
ir	5′-CGAAGTGGTGGTTATGCTGGAG-3′	5′-GGAGGCAATACGCTGGAACAAG-3′
irk2-RA	5′-ATGCGTTTCAATTTCTCCACCC-3′	5′-CTTGGTTTTCTGGCAAGTGAG-3′
irk2-RB	5′-GCTCAGCGATGTTCAGGTCCTG-3′	5′-CGTCGGCGAACACGTCTCATG-3′
irk2-RC	5′-ATGCGTTTCAATTTCTCCACCC-3′	5′-CTTGGTTTTCTGGCAAGTGAG-3′
irk3	5′-AAGTTCAGCGATAAGGCGGTG-3′	5′-TTTGGGCGTCGTAATGGATG-3′
rp49	5′-TGACCATCCGCCCAGCAT-3′	5′-TTCTTGGAGGAGACGCCGTG-3′

candidate genes for known transport and signalling functions and suggests new, previously unsuspected functions. Among the significant findings of this study was the observation that, of the very large K^+ channel gene family of *Drosophila*, all three of the inward rectifier *Drosophila* genes (*ir*, *irk2* and *irk3*) were both highly abundant and strongly enriched (to much greater extents than any other K^+ channels), clearly implicating inward rectifier potassium channels (IRKs) in epithelial function.

Mammalian IRKs form both homo- and hetero-tetramers and are sensitive to barium and to the antidiabetic sulphonylureas such as glibenclamide (Bryan and Aguilar-Bryan, 1997). Possible orthologues expressed in mammalian kidney include Kir6.x and Kir1.x. These channels are often associated with ABC transporters, such as cystic fibrosis transmembrane conductance regulator (CFTR) and sulphonylurea receptor (SUR), and complexes with these receptors render the channels more sensitive to glibenclamide (Ruknudin et al., 1998).

The highly upregulated expression pattern of the IRKs prompted our investigation into the effect of sulphonylureas on the Malpighian tubules. Not only do sulphonylureas inhibit fluid secretion, but glibenclamide blocks organic dye excretion by the tubule, and glibenclamide itself is both excreted and modified by the tubule.

Materials and methods

Drosophila

Oregon R flies were kept on standard medium in tubes at 25°C, 12 h:12 h photoperiod and 55% relative humidity. For dissection, flies were anaesthetized by chilling on ice and decapitated before dissecting out tubules in Schneider's medium (Invitrogen, Paisley, Scotland, UK). All chemicals and drugs were obtained from Sigma, unless otherwise stated.

Secretion assay

Fluid secretion assays were performed as described (Dow et al., 1994), taking readings every 10 min. Glibenclamide was added after the tubule basal secretion rate had been measured for 30 min. The secretion rate continued to be recorded for a further hour. Inhibition was calculated as the difference between the basal rate (measured over the first 30 min) and the secretion rate at 50 min. To study the effects of glibenclamide on neuropeptide-stimulated secretion, glibenclamide was added at 30 min, and the diuretic peptides *Drosophila* leucokinin (dLK; Radford et al., 2002; Terhzaz et al., 1999) and *Drosophila* corticotropin releasing factor-like peptide (dCRF, DH; Cabrero et al., 2002) were added at 60 min, then the secretion rate recorded for a further hour. In this way, the impact of sulphonylureas could be assessed both on resting and maximally stimulated fluid secretion.

Real-time quantitative PCR (qPCR)

qPCR was performed as described previously (McGettigan et al., 2005). Briefly, mRNA was prepared from 7-day-old Oregon R flies or their tubules using Qiagen RNAeasy column, following the manufacturer's methods (Qiagen, Crawley, West Sussex, UK). Reverse transcription was carried out using Superscript II (Invitrogen) using oligo-dT primer. For each sample, 500 ng of cDNA was added to 25 μl of SYBR Green reaction mix (Finnzymes, GRI, Braintree, Essex) and appropriate primers (Table 1). An Opticon 2 thermocycler (MJ Research, now Bio-Rad, Hemel Hempstead, Herts, UK) was set as follows; the recommended 15 min HotStart Taq activation time, then 40 cycles of (denaturing at 94°C for 30 s, annealing for 30 s at primer-dependent temperature, 30 s of extension at 72°C, and 10 s absorption reading at 80°C), followed by a 5 min final extension at 72°C and a melting curve from 70°C to 90°C. The ribosomal *rp49* gene was used as a standard in all experiments. Data were then expressed as fold difference of tubule cDNA compared with whole fly cDNA (± S.E.M.).

In situ *hybridization*

Tubules were dissected, fixed and subjected to *in situ* hybridization according to published protocols (Siviter et al., 2000) and the Berkeley *Drosophila* Genome Project (BDGP) 96-well *in situ* protocol (http://www.fruitfly.org/about/methods/RNAinsitu.html). *In situ* probes were directed towards the 3′ UTR of each gene to minimise cross-hybridisation between related genes. PCR products derived from the 3′ UTR of each gene were cloned into pBluescript or pCRII vectors (Invitrogen), and DIG-labelled RNA probes were generated by *in vitro* transcription. Adult tissues comprising gut, testes, ovaries and Malpighian tubules were dissected in Schneider's medium (Invitrogen) and placed into wells of a Millipore 96-well plate (MAGVN22 or MAGVS22) with 100 μl Schneider's medium. Schneider's medium was removed using a vacuum pump, and postfix solution [10 mmol l^{-1} potassium phosphate buffer (pH 7.0) containing 140 mmol l^{-1} NaCl, 0.1% Tween 20 and 5% v/v formaldehyde] was added for 20 min, followed by three washes with PBT [10 mmol l^{-1} potassium phosphate buffer (pH 7.0) containing

140 mmol l^{-1} NaCl and 0.1% v/v Tween 20]. The tissues were incubated with proteinase K in PBT (4 μg ml^{-1}) for 3 min at room temperature. The reaction was stopped with two washes of PBT containing 2 mg ml^{-1} glycine. The samples were washed twice with PBT before incubating with postfix for a further 20 min at room temperature. The tissues were washed with five changes of PBT, followed by one wash with 50% hybridisation buffer [5× SSC containing 50% v/v formamide, 10 mmol l^{-1} kPO_4, 140 mmol l^{-1} NaCl, 1 mg ml^{-1} glycogen, 0.2 mg ml^{-1} sheared salmon sperm DNA and 0.1% v/v Tween 20 (pH 7.0)] plus 50% PBT. The samples were washed once with hybridisation buffer, prior to a 1 h preincubation with hybridization buffer at 55°C, and subsequently incubated for 43 h at 55°C with 100 μl of hybridisation buffer containing 10–500 ng of either the sense or antisense riboprobe, taking care to seal the wells with Parafilm™ to prevent evaporation. Following hybridisation, the samples were washed four times with hybridization buffer at 55°C, followed by a final wash overnight with hybridization buffer at 55°C. Samples were washed once with 50% v/v hybridisation buffer and 50% v/v PBT, followed by four washes with PBT and then incubated overnight at room temperature with 100 μl of pre-absorbed alkaline phosphatase-conjugated anti-digoxigenin Fab fragment (Roche Molecular Biochemicals, Lewes, East Sussex, UK) diluted 1:2000 with PBT. The unbound antibody was removed with extensive washing in PBT (at least 10 times for ~5–10 min). The samples were incubated with DIG detection buffer [100 mmol l^{-1} Tris-HCl (pH 9.5), 100 mmol l^{-1} NaCl, 50 mmol l^{-1} $MgCl_2$] for 5 min then repeated again. The colour reaction was initiated by the addition of DIG detection buffer + 5-bromo-4-chloro-3-indolyl phosphate (BCIP) and nitroblue tetrazolium (NBT) and left for 10 min–2 h at room temperature. Development was stopped with extensive washing with PBT containing 50 mmol l^{-1} EDTA, and the tissues were removed from the wells, mounted on slides with 70% glycerol and viewed on an Axioscope microscope equipped with an Axiocam imaging system (Zeiss, Welwyn Garden City, UK).

Confocal imaging

Tubules were dissected and mounted on poly-lysine-coated slides in Schneider's medium. Glibenclamide labelled with Texas Red (Molecular Probes, now Invitrogen) was added to a final concentration of 0.1 mmol l^{-1}. A time series was generated under fluorescence with a Zeiss 510 Meta Confocal system. All images were taken at the same gain and exposure and processed using Axiovision 3.0.6 software.

Glibenclamide transport assays

Glibenclamide, at 10^{-6}–10^{-3} mol l^{-1}, was labelled with 0.05 μCi ^{125}I (Amersham Pharmacia, Amersham, UK, specific activity, 2000 Ci mmol l^{-1}) and added to tubule secretion assays, performed as described above. Secreted fluid was collected for 1 h, the volume measured and counted in Optiflow SAFE scintillant (Fisher Scientific UK, Loughborough, Leicestershire, UK). Transport ratios were calculated as the ratio of specific activities of secreted drop: reservoir bubble (values >1 thus imply concentration of the label by the tubule).

Thin layer chromatography (TLC)

Samples of 1 μl of both authentic [^{125}I]glibenclamide (0.05 μCi) and secreted fluid, obtained by the same method as the glibenclamide transport assay, were dried onto a 10×20 cm Polygram Sil G/UV254 plate (Machery-Nagel GmbH, Düren, Germany) and run out using an eluent of 85% v/v ethanol, 15% v/v PBS (pH 7) and 0.1% w/v SDS. Plates were visualized with a Fuji PhosphorImager.

Statistics

Where errors are shown, these represent the standard error of the mean (S.E.M.). Where appropriate, the significance of differences was tested with Student's *t*-test (two-tailed), taking a critical level of $P<0.05$.

Results

qPCR measurement of expression levels of Drosophila *IRKs*

Although microarray data provide a valuable first-pass survey of gene expression levels, it is prudent to validate array 'hits' independently before engaging in detailed study. The mean ratio results from qPCR analysis (Table 2) showed that all three IRK-encoding genes were enriched in tubule, compared with whole fly, cDNA, confirming previous Affymetrix microarray results (Wang et al., 2004). While the actual values produced from the qPCR and Affymetrix MAS5 analyses differ slightly, the relative levels between the genes are maintained; this represents further validation of the microarray dataset beyond the 12 genes originally subjected to qPCR (Wang et al., 2004).

One of these genes, *irk2*, was known to have two splice forms (Fig. 1), although the Affymetrix probes (against the 3′ end of the mRNA) would not have distinguished them. qPCR measurement allowed the identification of irk2-RA as the major transcript (Table 1). These results also suggested the presence of an additional splice form, verified by cloning and sequencing the PCR product. This new splice form, which will be denoted RC, has an extra 21 bases prior to the translated region of the RA splice form (Fig. 1). It appears to be a low-

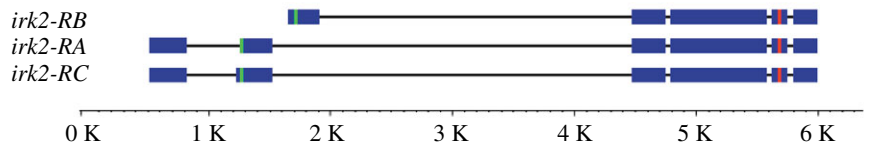

Fig. 1. Gene structure of *irk2*. Blue bars denote exons, green lines denote the start codons, and red lines denote the stop codons. The transcripts thus differ at their 5′ ends, and transcript B encodes a different protein from transcripts A and C. This display is based on the *Drosophila* genome annotation for *irk2* (www.flybase.org).

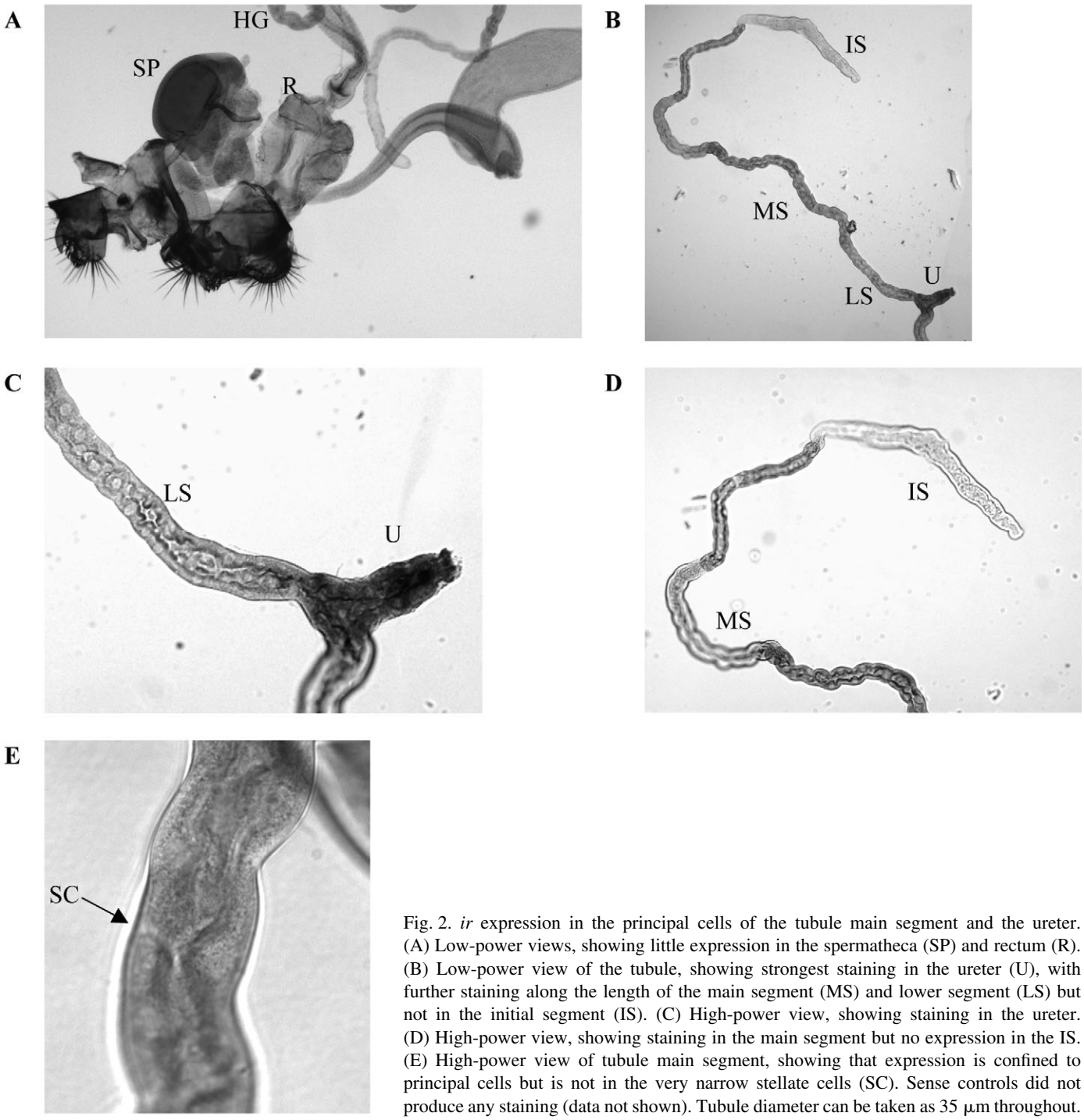

Fig. 2. *ir* expression in the principal cells of the tubule main segment and the ureter. (A) Low-power views, showing little expression in the spermatheca (SP) and rectum (R). (B) Low-power view of the tubule, showing strongest staining in the ureter (U), with further staining along the length of the main segment (MS) and lower segment (LS) but not in the initial segment (IS). (C) High-power view, showing staining in the ureter. (D) High-power view, showing staining in the main segment but no expression in the IS. (E) High-power view of tubule main segment, showing that expression is confined to principal cells but is not in the very narrow stellate cells (SC). Sense controls did not produce any staining (data not shown). Tubule diameter can be taken as 35 μm throughout.

abundance RNA product in the tubules, comprising only 6.2±0.6% of the expression of Irk2-RA. Irk2-RC did not reliably produce a qPCR product from the whole-fly cDNA because of its very low copy number. No other *D. melanogaster* IRK-encoding genes are known to have alternative splice forms.

Localisation of irk *gene expression in tubules*

In situ hybridisation confirmed that that all three IRKs were expressed abundantly in the tubule (Figs 2–4). The tubule is divided into six regions, with two predominant cell types (Sözen et al., 1997). For the most abundant and enriched gene, *irk3* (Table 2), there was widespread expression in all regions except the initial and transitional segments of the anterior tubules; interestingly, the equivalent regions of the posterior tubules stained throughout (Fig. 4). Additionally, within the main (secretory) segment of the tubule, only the principal cells and not the stellate cells expressed *irk3*. This is consistent with

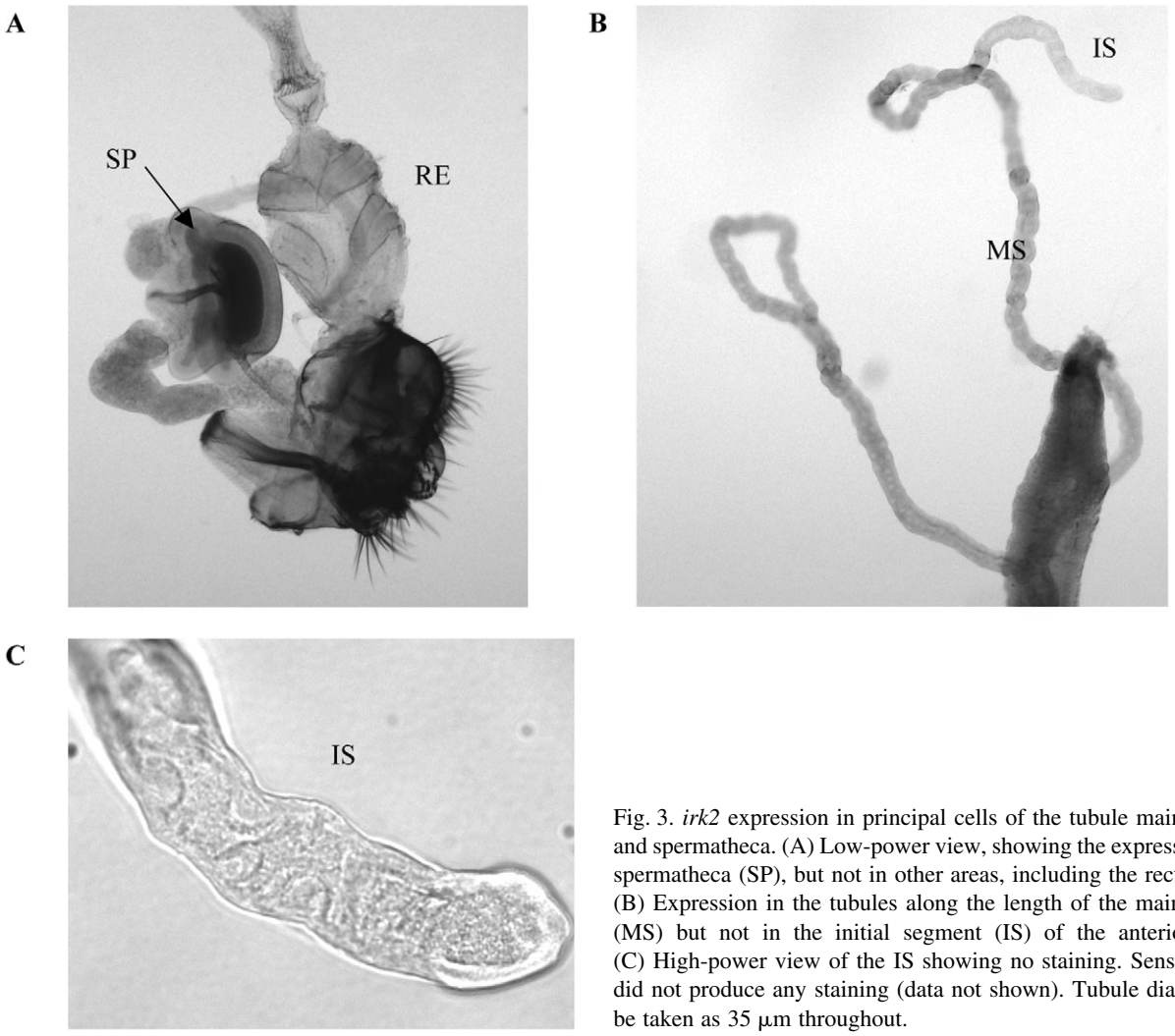

Fig. 3. *irk2* expression in principal cells of the tubule main segment and spermatheca. (A) Low-power view, showing the expression in the spermatheca (SP), but not in other areas, including the rectum (RE). (B) Expression in the tubules along the length of the main segment (MS) but not in the initial segment (IS) of the anterior tubule. (C) High-power view of the IS showing no staining. Sense controls did not produce any staining (data not shown). Tubule diameter can be taken as 35 μm throughout.

Table 2. *Microarray and qPCR data for the* irk *genes*

Gene	Microarray analysis*		qPCR	
	Tubule signal	Tubule:fly ratio	Tubule cT	Mean ratio
ir	1302±112	14.2±1.6	21.0±1.21	5.4±0.73
irk2-RA	527±33	5.7±0.24	17.3±0.38	9.2±3.23
irk2-RB			26.6±0.48	0.48±0.24
irk2-RC			23.0±0.40	>100†
irk3	2771±145	80.3±7.8	19.6±0.54	31.9±6.4

*Microarray analysis is from Wang et al. (2004). Note that the Affymetrix probe for *irk2* does not distinguish between the three *irk2* transcripts.

cT, threshold cycle.

†This ratio is approximate, because a quantitative real-time PCR (qPCR) signal could not be obtained consistently from whole-fly samples for *irk2*.

the principal cell being the major route for active potassium flux through the tubule: V-ATPases are also highly enriched in this cell type (Sözen et al., 1997), as in another dipteran, *Aedes aegypti* (Weng et al., 2003). Irk3 was also observed in developing oocytes (Fig. 4F).

The other two genes gave fainter signals, but both were still clearly expressed in tubule principal cells. However, *ir* was most abundantly expressed in the ureter (Fig. 2), whereas *irk2* was most abundant in spermatheca (Fig. 3A). It is thus clear that, although all genes contribute to main segment function, *ir* and *irk3* are also found in lower tubule, a region associated with fluid reabsorption (O'Donnell and Maddrell, 1995). IRKs may thus play a role both in secretion and reabsorption in distinct spatial regions of the tubule. As the genes are extensively co-expressed in the tubule, and as IRKs can form hetero-tetramers, there is a possibility that the properties of the channels *in vivo* may not resemble those measured by heterologous expression *in vitro* (Doring et al., 2002).

As the electrochemical gradient at the apical membrane does not favour net K^+ secretion (Beyenbach et al., 2000), it is also likely that IRKs will be located on the basolateral membrane. Could they then constitute a major route for K^+ entry?

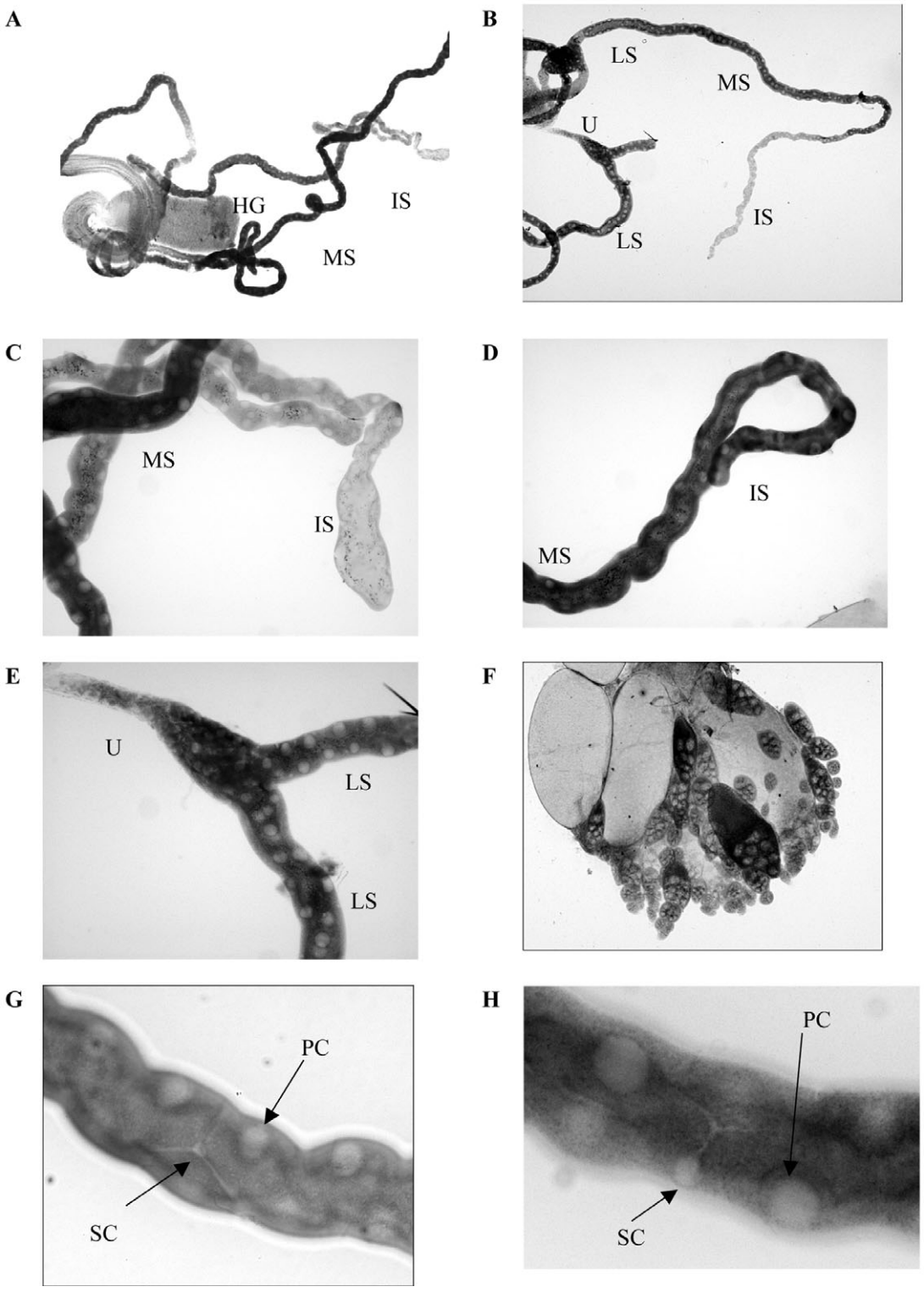

Fig. 4. *irk3* expression is localised to the principal cells of the tubule main segment by *in situ* analysis. (A,B) Low-power views, showing expression in the main segment (MS), lower segment (LS) and ureter (U) of the tubule but not in the initial segment (IS) of the anterior tubule or the hindgut (HG). (C) High-power view of the anterior tubule initial segment, showing no expression. By contrast, the initial segment of the posterior tubule (D) shows staining as intense as the main segment. (E) High-power view of the lower tubule and ureter, showing expression throughout. (F) High levels of expression in nurse cells and oocytes. (G,H) High-power view of tubule main segment, showing that expression is confined to principal cells (PC) but is not in the very narrow stellate cells (SC). The two cell types can be distinguished because stellate cell nuclei are smaller than those of principal cells (arrows). Sense controls did not produce any staining (data not shown). Tubule diameter can be taken as 35 μm throughout.

Sulphonylureas block fluid secretion

The cardinal inhibitors of IRKs are the antidiabetic sulphonylureas such as glibenclamide (Inagaki et al., 1996). Consistent with a major role for IRKs in tubule, fluid secretion was found to be inhibited by sulphonylureas. Glibenclamide inhibited fluid secretion with an IC_{50} of 0.78±0.03 mmol l^{-1} (Fig. 5). Maximal inhibition was observed 20–40 min after the drug was added, depending on concentration. The IC_{50} value is comparable with those found in mammalian Kir1.1 channels in the absence of SUR2B (Konstas et al., 2002) and *Tenebrio molitor* tubules (Wiehart et al., 2003).

To characterize the sulphonylurea sensitivity of the tubule further, tolbutamide, minoxidil and diazoxide were also tested and shown to inhibit secretion (Fig. 6). Approximate IC_{50} values for these drugs were estimated as 5 mmol l^{-1}, 0.01 mmol l^{-1} and 0.1 mmol l^{-1}, respectively. Tolbutamide has a lower binding efficiency to SURs than glibenclamide (Dorschner et al., 1999) and is often shown to require approximately 10 times the concentration of glibenclamide in order to produce the same effects. Although Minoxidil is a potassium channel activator, it has also been shown to decrease urine produce in humans (Wang, 2003), as was found here. It is thus clear that tubule secretion is inhibited by a range of sulphonylureas, with very similar pharmacology to humans. On balance, however, the relatively high IC_{50}s suggest that either the tubule IRKs are of the lower affinity class that do not need to associate closely with an SUR or that there are additional targets for sulphonylureas in tubule.

SUR may not be associated with IRKs in tubule

Diflubenzuron is a competitor for glibenclamide binding to SUR in *Drosophila* (Abo-Elghar et al., 2004). In secretion assays where diflubenzuron was added, followed 30 min later by glibenclamide, no change in secretion rate was observed (Fig. 7). Inhibition by glibenclamide was unaffected, suggesting that glibenclamide is not binding to SUR. Microarray results (Wang et al., 2004) showed that SUR was not abundant in the Malpighian tubule; however, it was envisaged that there might be a functional homologue. The results from the diflubenzuron and IC_{50} experiments suggest that the IRK channels in the tubule do not form complexes similar to the Kir6.x/SUR complexes in mammals, although they do not exclude the possibility that glibenclamide is acting on a target distinct from IRK, such as CFTR. However, no *Drosophila* orthologues for CFTR were identified in a survey of *Drosophila* ABC transporters (Dean et al., 2001).

Amaranth secretion is inhibited by glibenclamide

Amaranth, an innocuous red food dye, was observed to be concentrated in secreted fluid (Maddrell and Gardiner, 1975) and is widely used to help view the secreted bubbles in secretion assays (Dow et al., 1994); however, the mechanism of active amaranth secretion is unknown. During the secretion assay, amaranth transport was observed to be inhibited by glibenclamide. Amaranth transport was abolished after 35 min

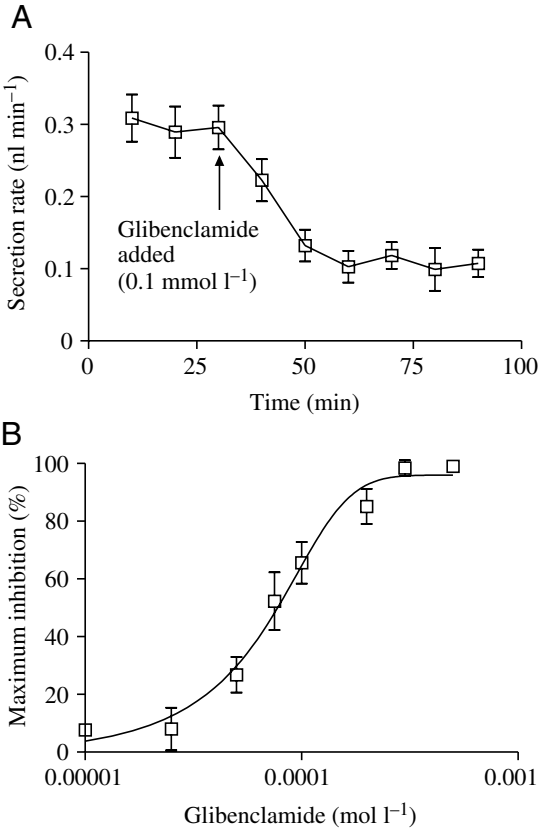

Fig. 5. Inhibition of fluid secretion by glibenclamide. (A) Typical experiment showing secretion response (means ± S.E.M., *N*=13) to glibenclamide. (B) Dose–response curve; inhibition relative to control was calculated 50 min after glibenclamide was added (data are expressed as mean percentage inhibition ± S.E.M., *N*=7).

when the concentration of glibenclamide was greater than 0.1 mmol l^{-1}, and some inhibition was observed above 0.01 mmol l^{-1} (Fig. 8). Inhibition of amaranth transport thus occurs at glibenclamide concentrations tenfold lower than the IC_{50} for glibenclamide action on fluid secretion, and so shows that the two effects are independent actions of glibenclamide. Glibenclamide was further found to block Orange R and Phenol Red transport (data not shown). The inhibition of amaranth transport suggested that glibenclamide may be preferentially transported *via* the same mechanism as amaranth.

Further secretion assays demonstrated that Phenol Red and amaranth did not impact on the inhibition of fluid secretion by glibenclamide. In secretion assays where no dye was added to the reservoir bubble, the reduction of secretion caused by glibenclamide was not significantly different (Fig. 9).

Glibenclamide is both transported and metabolized by tubule

The serendipitous observation that glibenclamide blocked the transport of a wide range of organic dyes by tubule suggested a second action of sulphonylureas in tubule; an impact on organic solute transporters. We hypothesized that this might reflect competition for the same excretory

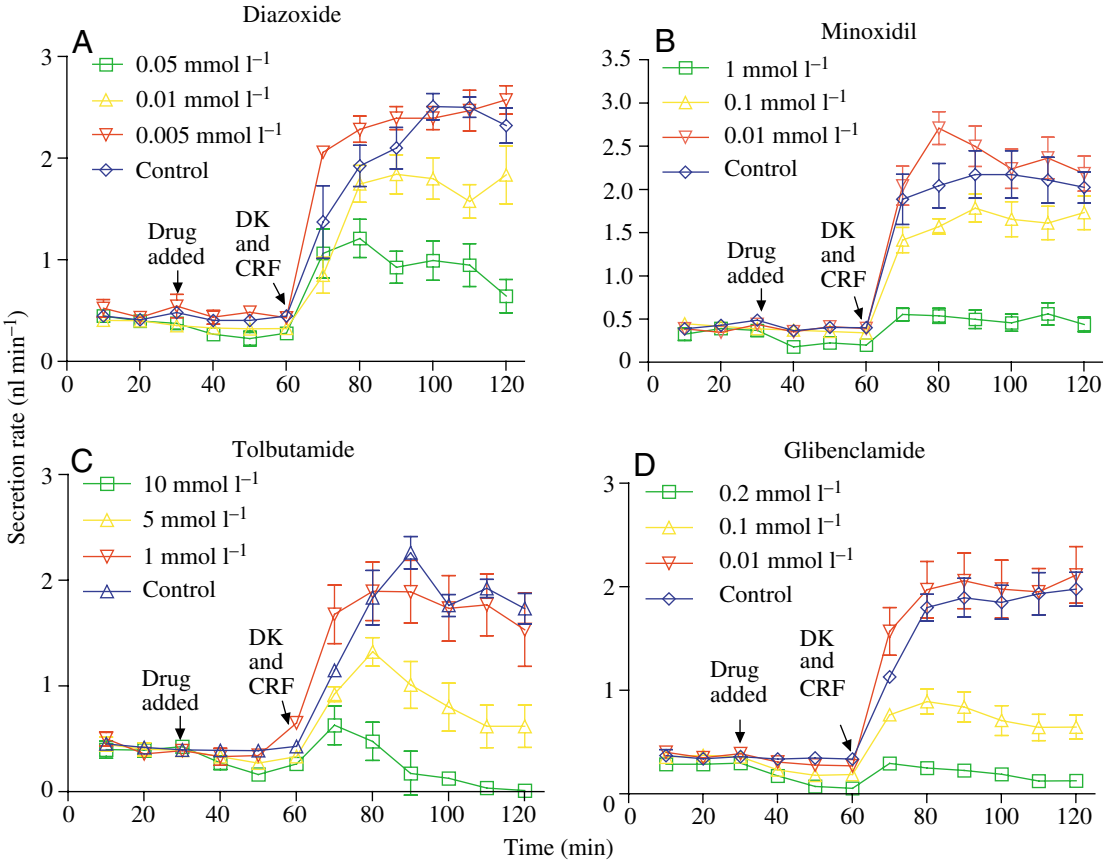

Fig. 6. Inhibition of secretion by a range of sulphonylureas. (A) Diazoxide, (B) minoxidil, (C) tolbutamide or (D) glibenclamide were added after 30 min. *Drosophila* corticotropin releasing factor-like peptide (dCRF) and *Drosophila* leucokinin (dLK) were added (to final concentrations of 10^{-7} mol l^{-1}) after a further 30 min to stimulate the secretion rate. Secretion rates are shown as means ± S.E.M. (N=7).

transporters; tubules are known to express a huge repertoire of broad-specificity solute transporters (Wang et al., 2004). Accordingly, possible transport of glibenclamide was observed using confocal microscopy. The fluorescent glibenclamide appeared initially to adhere to the basolateral membrane, before entering the cells (Fig. 10). The fluorescent glibenclamide was observed in the cytoplasm of the principal cells; this occurs along the length of the tubule. The basolateral border between the principal cell and stellate cells also showed up clearly. There was a particularly strong signal from the initial segment of the anterior tubules, a region that does not contribute to fluid secretion (O'Donnell and Maddrell, 1995) but that actively excretes calcium (Dube et al., 2000). At the urethra, fluorescent secreted bubbles were visible.

The nature of the glibenclamide transport was investigated further using I^{125}-labelled glibenclamide. Measurements of the radioactivity in the secreted drops and reservoir bubbles revealed that the level of radioactivity was approximately 8-fold higher than the bathing solution in the secreted drops across all glibenclamide concentrations investigated (Fig. 11B). The rate of secretion rose with the glibenclamide concentration (Fig. 11A). The rate and ratio measurements show that glibenclamide transport certainly occurs and that the mechanism was saturated at the highest concentration we were

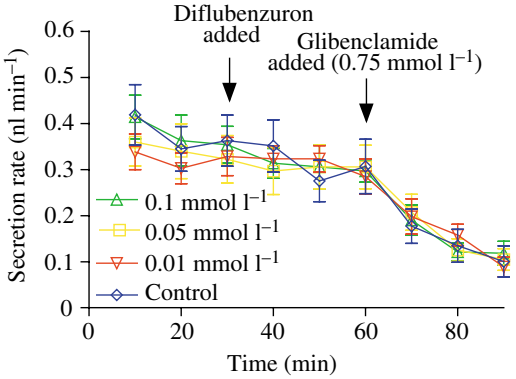

Fig. 7. Effect of diflubenzuron on secretion and glibenclamide inhibition. Diflubenzuron was added to the final concentrations shown after 30 min. Glibenclamide (final concentration 0.75 mmol l^{-1}) was added 30 min later. Secretion rates are shown as means ± S.E.M. (N=8).

able to employ. Thin layer chromatography (TLC) on the secreted and original radiolabelled glibenclamide showed that the secreted glibenclamide was modified (Fig. 11C). This modification precludes the conclusion that glibenclamide is actively transported, as we cannot confirm the existence of transport across an adverse electrochemical gradient. However,

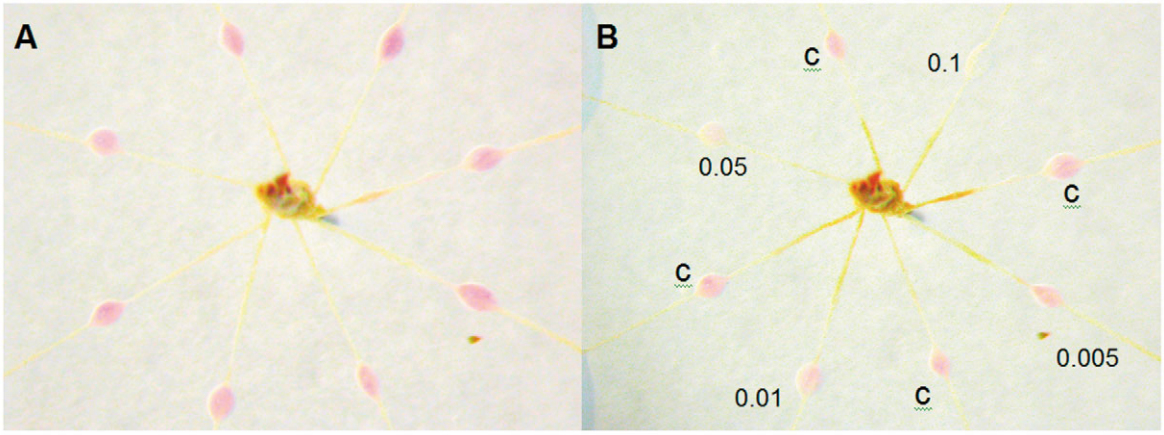

Fig. 8. Glibenclamide blocks amaranth transport. Eight tubules were arranged radially for classical (Ramsay) secretion assays (Dow et al., 1994): the bathing drops are just out of shot. Droplets were collected every 10 min, and so the colour of the droplets provides a correlate of real-time amaranth transport. (A) Secreted drops before glibenclamide was added. (B) Secreted droplets 35 min after glibenclamide was added to the final concentrations (in mmol l^{-1}) shown. Drops labelled 'C' had no glibenclamide added to the bubbles. The concentration of amaranth in the reservoir bubbles was 2 μmol l^{-1}.

for practical purposes, glibenclamide is rapidly and avidly removed from the basolateral surface of the cell.

Glibenclamide inhibition mimics the effect of K^+-free saline

Glibenclamide, although a classical inhibitor of IRKs, has also been shown to act on a wide range of targets. For example, it blocks ABC transporters other than SUR, such as CFTR (Zhang et al., 2004). It has been argued to affect L-type calcium channels and the Na^+/K^+-ATPase (Lee and Lee, 2005) and to induce a chloride conductance in mitochondria that collapses the inner membrane potential (Fernandes et al., 2004). So, it is premature to ascribe the potent inhibition of tubule secretion by glibenclamide to blockade of IRKs. However, our confidence is increased by the fact that a range of sulphonylureas, and not just glibenclamide, are effective (Fig. 6). Is it possible to go further?

The effects of glibenclamide were compared with exposure of the tubule to K^+-free saline. *Drosophila* tubule secretion has been reported to persist for some hours in K^+-free saline (Linton and O'Donnell, 1999), so if the action of glibenclamide was at a site distinct from IRKs, then secretion in K^+-free saline should still be sensitive to glibenclamide. However, in our experiments, K^+-free saline led to a total inhibition of fluid secretion, with a time course very similar to that of glibenclamide addition, and so glibenclamide has no further effect on tubules in K^+-free saline (Fig. 12). We thus consider that the action of glibenclamide is consistent with a run-down of cellular K^+, similar to that produced by removing external K^+, although, given the multiple potential targets of glibenclamide, we cannot rule out more complex possibilities.

Discussion

Microarray analysis is a potent tool, but all the more so when it directs downstream functional analysis. Fortunately, the *Drosophila* renal tubule is an ideal tissue for such study.

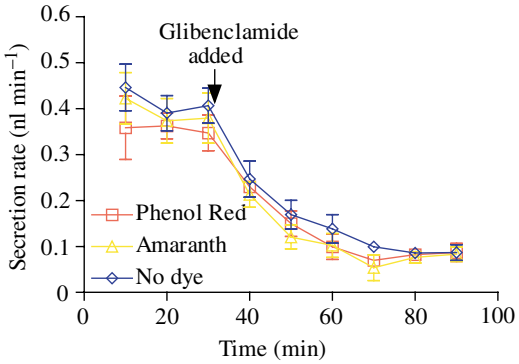

Fig. 9. Anionic dyes do not impact on glibenclamide inhibition of fluid secretion. Classical secretion assays were performed in normal medium or with the addition of phenol red (2×10^{-5} mol l^{-1}) or amaranth (2×10^{-5} mol l^{-1}). Glibenclamide (final concentration 10^{-4} mol l^{-1}) was added after 30 min. Secretion rates are shown as means ± S.E.M. (N=6).

Microarray analysis clearly implicated IRKs in tubule function, and this paper has confirmed the abundance and enrichment of mRNAs for all three *Drosophila* IRKs and further localised them to the principal cell, which is known to be the site of active electrogenic cation transport. This builds on previous *in situ* data, which have variously described *ir* as widely expressed (MacLean et al., 2002), especially in embryonic salivary gland, and localises *irk2* to embryonic hindgut and *irk3* to embryonic Malpighian tubules (Doring et al., 2002). Our data show that, in adults, all three IRKs are present in tubule. As IRKs form both homo- and hetero-tetramers (Bryan and Aguilar-Bryan, 1997), there is thus ample scope for sophistication in tubule K^+ channel expression. Interestingly, the three IRKs show overlapping, but distinct, patterns of expression; *irk3* is expressed in main segment principal cells and lower tubule, implying a role in both fluid secretion and reabsorption.

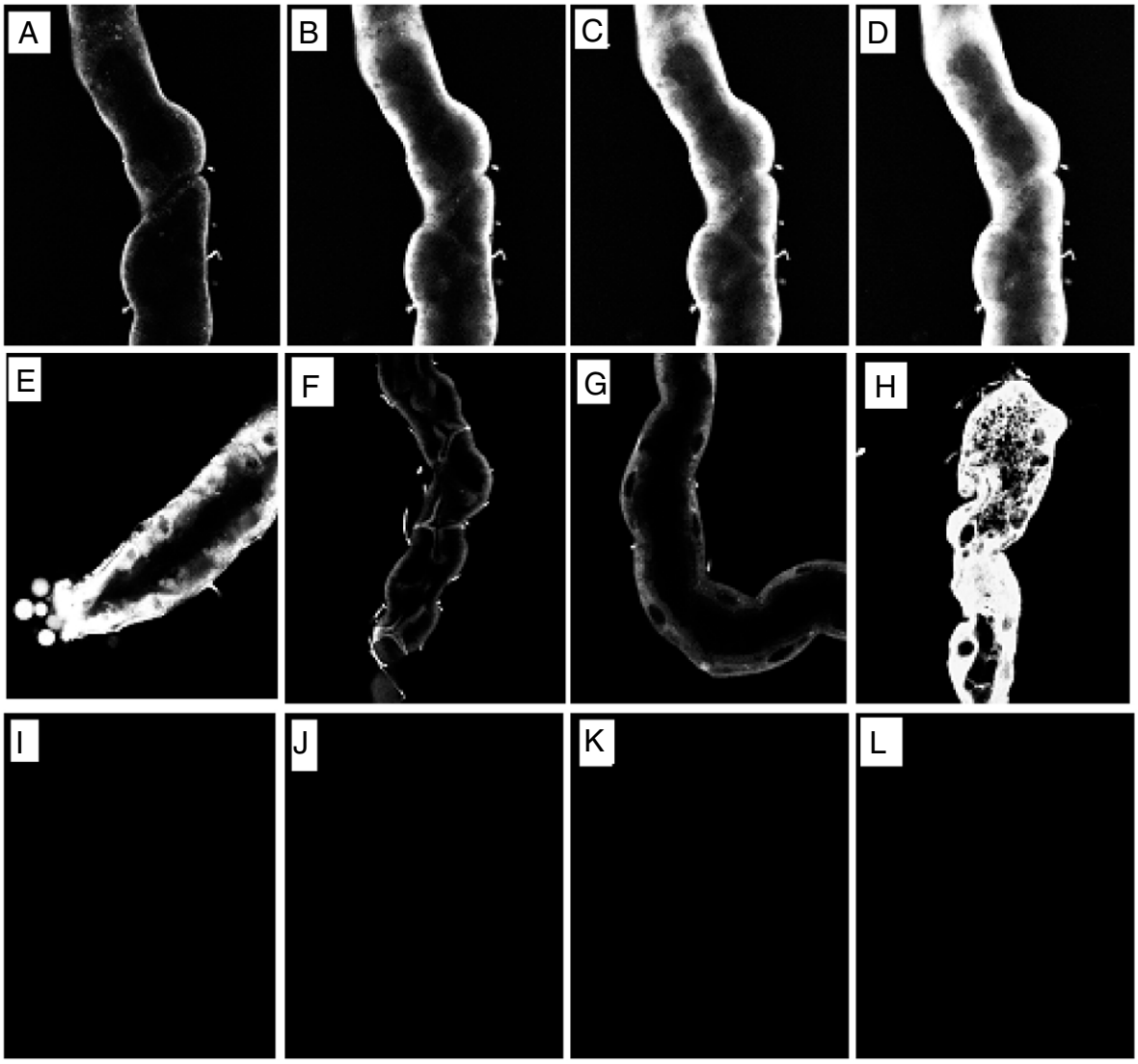

Fig. 10. Transport of fluorescent glibenclamide. Tubules were dissected and incubated in medium containing Texas Red (TR)-labelled glibenclamide. (A–D) Images taken from a time series at 1 min, 15 min, 30 min and 45 min, respectively. Panels E–L show features of glibenclamide transport in specific areas of the tubule: (E) urethra; (F) surface of the main segment, showing the stellate cells; (G) main segment; (H) initial segment of anterior tubule. Images A–D were taken 40 min after the addition of 0.1 mmol l^{-1} TR-glibenclamide. Images I–L were taken of the same regions of the tubule as E–H but were not exposed to TR-glibenclamide. The same detector gain (0.01) and off-set amplification (500) were used for all images. Tubule diameters can be taken as 35 μm throughout.

As would be expected, fluid secretion was shown to be sensitive to a wide range of the antidiabetic sulphonylureas that are selective inhibitors of IRKs in vertebrates. The sensitivity to these drugs, however, was not sufficiently high to suggest that these IRKs are associated with *Drosophila* SUR or a related ABC transporter; in support of this, a known inhibitor of *Drosophila* SUR had no effect on fluid secretion. However, it was possible to completely inhibit fluid secretion with sulphonylureas (Fig. 6), whereas inhibitors of Na^+/K^+-ATPase and $Na^+/K^+/2Cl^-$ co-transport achieve only partial inhibition of fluid secretion (Ianowski and O'Donnell, 2004; Torrie et al., 2004), and so, with this broad panel of selective inhibitors, we can confidently assert a major role for IRKs in tubule.

Do IRKs participate in basolateral entry of K^+?

The extraordinary abundance of mRNA for *ir*, *irk2* and *irk3* in tubule (Wang et al., 2004; Table 2) suggests an important role for these channels. The sulphonylurea pharmacology, although less conclusive, shows a similar effect to K^+-free saline, suggesting a possible role for IRKs in the entry step. This is consistent with many models for tubule function, in which basolateral K^+ channels have featured (Beyenbach et al., 2000; Dow and Davies, 2003; Wiehart et al., 2003). However, important basolateral roles have also been shown both for $Na^+/K^+/2Cl^-$ co-transport and the Na^+/K^+-ATPase (Ianowski and O'Donnell, 2004; Torrie et al., 2004), and a small (9 mV) outward electrochemical gradient for K^+ has been shown for

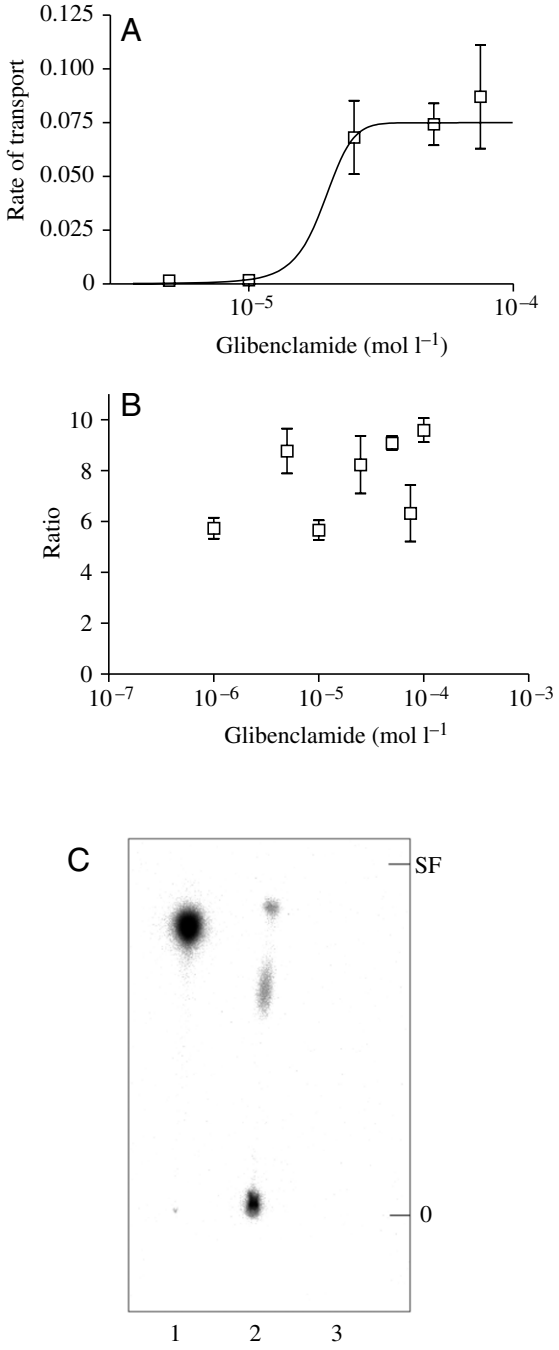

Fig. 11. Transport and metabolism of ^{125}I-labelled glibenclamide. (A) Transport rates and (B) secreted:bathing ratios of [^{125}I]glibenclamide at different bathing glibenclamide concentrations. (C) Thin-layer chromatography plate image. Lane 1, authentic [^{125}I]glibenclamide; lane 2, secreted drop after [^{125}I]glibenclamide was added to the bathing solution; lane 3, secreted drop where no radiolabelled glibenclamide was added. Lower and upper bars represent the origin and solvent front, respectively.

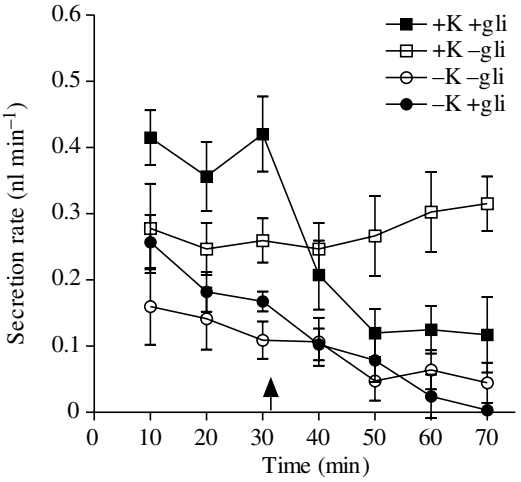

Fig. 12. Glibenclamide mimics the effect of K^+-free saline. Tubules were dissected in AARS saline (a defined control saline; Linton and O'Donnell, 1999), then either mounted for fluid secretion directly in 10 μl drops of AARS saline or rinsed and mounted for secretion in drops of K^+-free saline (Linton and O'Donnell, 1999). Readings were taken every 10 min. At 30 min (arrow), glibenclamide was added (to a final concentration of 0.1 mmol l^{-1}) to half of the AARS and half of the K^+-free drops. Key: open squares, control saline without glibenclamide; filled squares, control saline with glibenclamide; open circles, K^+-free saline without glibenclamide; filled circles, K^+-free saline with glibenclamide. Data are shown as means ± S.E.M. (*N*=8).

the basolateral membrane of resting *Drosophila* tubule (Ianowski and O'Donnell, 2004). Can this conflicting data be reconciled? We suggest that IRKs play only a minor role in basal secretion: their rectification properties imply that they are unlikely to let much K^+ out, down its electrochemical gradient. However, when the tubule is maximally stimulated, and the apical electrogenic V-ATPase is driving K^+ exit across the apical membrane, we suggest that basolateral IRKs allow K^+ entry to support the active apical membrane. IRKs could thus be seen as adaptations to facilitate the remarkably high per-cell secretion rates that seem to be characteristic of insect tubules (Dow and Davies, 2003; Maddrell, 1991). Consistent with this, all the sulphonylureas showed a more marked effect on stimulated, rather than basal, fluid secretion (Fig. 6).

Transport and metabolism of glibenclamide

We also observed two novel effects of glibenclamide: (1) the tubule itself both excretes and modifies the compound and (2) glibenclamide inhibits the excretion of a range of organic dyes. Although the sulphonylureas are valuable human therapeutic agents, the molecular mechanisms of their clearance are not understood in detail; for example, it is not clear whether SUR is itself a sulphonylurea transporter. However, our results may impinge on clearance mechanisms. Although we did not rigorously show competition between these solutes, it would be a very plausible explanation, and this paper does identify a range of interesting dyes that may help in such studies.

Demonstration of glibenclamide transport further raises the possibility that the apparent IC_{50}s for sulphonylureas may be distorted by rapid removal from the basolateral membrane infoldings of the principal cell, as has been shown for ouabain

(Torrie et al., 2004). This would have the effect of protecting basolateral IRKs by only exposing them to a concentration of sulphonylureas that was significantly lower than the macroscopic bath concentration, thus producing anomalously high IC_{50}s. We have not yet identified an inhibitor of glibenclamide transport, so we cannot unmask a higher affinity effect of glibenclamide, as was possible for ouabain (Torrie et al., 2004). We must thus be cautious about asserting an accurate IC_{50} for glibenclamide; this will need to be established by heterologous expression in culture, where such confounding elements do not appear.

Phylogenetic scope of the model

Comparison of the *Drosophila* and *Anopheles* genome projects reveal that IRKs are very similar between these dipteran species; indeed, there appears to have been a gene expansion in *Anopheles* (McCormack, 2003). Glibenclamide sensitivity (at relatively high concentrations: 5 mmol l^{-1}) has also been documented in *Tenebrio molitor*, a beetle (Wiehart et al., 2003). In *Tenebrio*, the effect of glibenclamide was similar to that of barium, another characteristic of IRKs. Barium sensitivity has also been widely documented in tubules of *Drosophila* (Ianowski and O'Donnell, 2004; Wessing et al., 1993), the locust *Schistocerca gregaria* (Hyde et al., 2001) and the yellow fever mosquito, *Aedes aegypti* (Beyenbach and Masia, 2002) Consistent with this, *Drosophila* IRKs reveal weak barium sensitivity when expressed heterologously in S2 cells (Doring et al., 2002). Our results, showing sensitivity of fluid secretion to a spectrum of sulphonylurea antidiabetics, and localising all three IRKs to the same cell type as the apical V-ATPase, may thus have broad scope.

This work was supported by a studentship and grants from the UK's Biotechnology and Biological Sciences Research Council (BBSRC). We are grateful to Dr C. T. Brett for the loan of thin layer chromatography equipment. We would like to thank a referee for suggesting the K^+-free experiment.

References

Abo-Elghar, G. E., Fujiyoshi, P. and Matsumura, F. (2004). Significance of the sulfonylurea receptor (SUR) as the target of diflubenzuron in chitin synthesis inhibition in *Drosophila melanogaster* and *Blattella germanica*. *Insect Biochem. Mol. Biol.* **34**, 743-752.

Beyenbach, K. W. and Masia, R. (2002). Membrane conductances of principal cells in Malpighian tubules of *Aedes aegypti*. *J. Insect Physiol.* **48**, 375-386.

Beyenbach, K. W., Pannabecker, T. L. and Nagel, W. (2000). Central role of the apical membrane H^+-ATPase in electrogenesis and epithelial transport in Malpighian tubules. *J. Exp. Biol.* **203**, 1459-1468.

Bryan, J. and Aguilar-Bryan, L. (1997). The ABCs of ATP-sensitive potassium channels: more pieces of the puzzle. *Curr. Opin. Cell Biol.* **9**, 553-559.

Cabrero, P., Radford, J. C., Broderick, K. E., Costes, L., Veenstra, J. A., Spana, E. P., Davies, S. A. and Dow, J. A. T. (2002). The *Dh* gene of *Drosophila melanogaster* encodes a diuretic peptide that acts through cyclic AMP. *J. Exp. Biol.* **205**, 3799-3807.

Dean, M., Rzhetsky, A. and Allikmets, R. (2001). Human and *Drosophila* ABC proteins. In *ABC Proteins From Bacteria To Man* (ed. B. Holland, S. P. Cole, K. Kuchler and C. F. Higgins), pp. 47-61. London: Academic Press.

Denholm, B., Sudarsan, V., Pasalodos-Sanchez, S., Artero, R., Lawrence, P., Maddrell, S., Baylies, M. and Skaer, H. (2003). Dual origin of the renal tubules in *Drosophila*: mesodermal cells integrate and polarize to establish secretory function. *Curr. Biol.* **13**, 1052-1057.

Doring, F., Wischmeyer, E., Kuhnlein, R. P., Jackle, H. and Karschin, A. (2002). Inwardly rectifying K^+ (Kir) channels in *Drosophila*. A crucial role of cellular milieu factors Kir channel function. *J. Biol. Chem.* **277**, 25554-25561.

Dorschner, H., Brekardin, E., Uhde, I., Schwanstecher, C. and Schwanstecher, M. (1999). Stoichiometry of sulfonylurea-induced ATP-sensitive potassium channel closure. *Mol. Pharmacol.* **55**, 1060-1066.

Dow, J. A. T. and Davies, S. A. (2001). The *Drosophila melanogaster* Malpighian tubule. *Adv. Insect Physiol.* **28**, 1-83.

Dow, J. A. T. and Davies, S. A. (2003). Integrative physiology and functional genomics of epithelial function in a genetic model organism. *Physiol. Rev.* **83**, 687-729.

Dow, J. A. T., Maddrell, S. H. P., Görtz, A., Skaer, N. V., Brogan, S. and Kaiser, K. (1994). The Malpighian tubules of *Drosophila melanogaster*: a novel phenotype for studies of fluid secretion and its control. *J. Exp. Biol.* **197**, 421-428.

Dow, J. A. T., Kelly, D. C., Davies, S. A., Maddrell, S. H. P. and Brown, D. (1995). A novel member of the major intrinsic protein family in *Drosophila* – are aquaporins involved in insect Malpighian (renal) tubule fluid secretion? *J. Physiol.* **489**, P110-P111.

Dube, K., McDonald, D. G. and O'Donnell, M. J. (2000). Calcium transport by isolated anterior and posterior Malpighian tubules of Drosophila melanogaster: roles of sequestration and secretion. *J. Insect Physiol.* **46**, 1449-1460.

Fernandes, M. A., Santos, M. S., Moreno, A. J., Duburs, G., Oliveira, C. R. and Vicente, J. A. (2004). Glibenclamide interferes with mitochondrial bioenergetics by inducing changes on membrane ion permeability. *J. Biochem. Mol. Toxicol.* **18**, 162-169.

Hyde, D., Baldrick, P., Marshall, S. L. and Anstee, J. H. (2001). Rubidium reduces potassium permeability and fluid secretion in Malpighian tubules of *Locusta migratoria*, L. *J. Insect Physiol.* **47**, 629-637.

Ianowski, J. P. and O'Donnell, M. J. (2004). Basolateral ion transport mechanisms during fluid secretion by *Drosophila* Malpighian tubules: Na^+ recycling, Na^+:K^+:2Cl^- cotransport and Cl^- conductance. *J. Exp. Biol.* **207**, 2599-2609.

Inagaki, N., Gonoi, T., Clement, J. P., Wang, C. Z., Aguilar-Bryan, L., Bryan, J. and Seino, S. (1996). A family of sulfonylurea receptors determines the pharmacological properties of ATP-sensitive K^+ channels. *Neuron* **16**, 1011-1017.

Kaufmann, N., Kean, L., Mathai, J., Hill, W., Dow, J. A. T., Zeidel, M. and Brodsky, J. (2004). Fluid secretion and solute transport in *Drosophila*. *A. Dros. Res. Conf.* **45**, 653B.

Konstas, A. A., Dabrowski, M., Korbmacher, C. and Tucker, S. J. (2002). Intrinsic sensitivity of Kir1.1 (ROMK) to glibenclamide in the absence of SUR2B. Implications for the identity of the renal ATP-regulated secretory K^+ channel. *J. Biol. Chem.* **277**, 21346-21351.

Lee, S. Y. and Lee, C. O. (2005). Inhibition of Na^+-K^+ pump and L-type Ca^{2+} channel by glibenclamide in guinea pig ventricular myocytes. *J. Pharmacol. Exp. Ther.* **312**, 61-68.

Linton, S. M. and O'Donnell, M. J. (1999). Contributions of K^+:Cl^- cotransport and Na^+/K^+-ATPase to basolateral ion transport in Malpighian tubules of *Drosophila melanogaster*. *J. Exp. Biol.* **202**, 1561-1570.

MacLean, S. J., Andrews, B. C. and Verheyen, E. M. (2002). Characterization of Dir: a putative potassium inward rectifying channel in *Drosophila*. *Mech. Dev.* **116**, 193-197.

Maddrell, S. H. P. (1991). The fastest fluid-secreting cell known: the upper Malpighian tubule cell of *Rhodnius*. *BioEssays* **13**, 357-362.

Maddrell, S. H. and Gardiner, B. O. (1975). Induction of transport of organic anions in Malpighian tubules of *Rhodnius*. *J. Exp. Biol.* **63**, 755-761.

Masia, R., Aneshansley, D., Nagel, W., Nachman, R. J. and Beyenbach, K. W. (2000). Voltage clamping single cells in intact Malpighian tubules of mosquitoes. *Am. J. Physiol. Renal Physiol.* **279**, F747-F754.

McCormack, T. J. (2003). Comparison of K^+-channel genes within the genomes of *Anopheles gambiae* and *Drosophila melanogaster*. *Genome Biol.* **4**, R58.

McGettigan, J., McLennan, R. K. J., Broderick, K. E., Allan, A. K., Cabrero, P., Regulski, M. R., Pollock, V. P., Gould, G. W., Davies, S. A. and Dow, J. A. T. (2005). Insect renal tubules constitute a cell-autonomous immune system that protects the organism against bacterial infection. *Insect Biochem. Mol. Biol.* **35**, 741-754.

McNicholas, C. M., Guggino, W. B., Schwiebert, E. M., Hebert, S. C.,

Giebisch, G. and Egan, M. E. (1996). Sensitivity of a renal K^+ channel (ROMK2) to the inhibitory sulfonylurea compound glibenclamide is enhanced by coexpression with the ATP-binding cassette transporter cystic fibrosis transmembrane regulator. *Proc. Natl. Acad. Sci. USA* **93**, 8083-8088.

O'Donnell, M. J. and Maddrell, S. H. P. (1995). Fluid reabsorption and ion transport by the lower Malpighian tubules of adult female *Drosophila*. *J. Exp. Biol.* **198**, 1647-1653.

O'Donnell, M. J., Dow, J. A. T., Huesmann, G. R., Tublitz, N. J. and Maddrell, S. H. P. (1996). Separate control of anion and cation transport in Malpighian tubules of *Drosophila melanogaster*. *J. Exp. Biol.* **199**, 1163-1175.

Radford, J. C., Davies, S. A. and Dow, J. A. T. (2002). Systematic GPCR analysis in *Drosophila melanogaster* identifies a leucokinin receptor with novel roles. *J. Biol. Chem.* **277**, 38810-38817.

Ruknudin, A., Schulze, D. H., Sullivan, S. K., Lederer, W. J. and Welling, P. A. (1998). Novel subunit composition of a renal epithelial KATP channel. *J. Biol. Chem.* **273**, 14165-14171.

Siviter, R. J., Coast, G. M., Winther, A. M., Nachman, R. J., Taylor, C. A., Shirras, A. D., Coates, D., Isaac, R. E. and Nassel, D. R. (2000). Expression and functional characterization of a *Drosophila* neuropeptide precursor with homology to mammalian preprotachykinin A. *J. Biol. Chem.* **275**, 23273-23280.

Sözen, M. A., Armstrong, J. D., Yang, M. Y., Kaiser, K. and Dow, J. A. T. (1997). Functional domains are specified to single-cell resolution in a *Drosophila* epithelium. *Proc. Natl. Acad. Sci. USA* **94**, 5207-5212.

Terhzaz, S., O'Connell, F. C., Pollock, V. P., Kean, L., Davies, S. A., Veenstra, J. A. and Dow, J. A. T. (1999). Isolation and characterization of a leucokinin-like peptide of *Drosophila melanogaster*. *J. Exp. Biol.* **202**, 3667-3676.

Torrie, L. S., Radford, J. C., Southall, T. D., Kean, L., Dinsmore, A. J., Davies, S. A. and Dow, J. A. T. (2004). Resolution of the insect ouabain paradox. *Proc. Natl. Acad. Sci. USA* **101**, 13689-13693.

Wang, J., Kean, L., Yang, J., Allan, A. K., Davies, S. A., Herzyk, P. and Dow, J. A. T. (2004). Function-informed transcriptome analysis of *Drosophila* renal tubule. *Genome Biol.* **5**, R69.

Wang, T. (2003). The effects of the potassium channel opener minoxidil on renal electrolytes transport in the loop of henle. *J. Pharmacol. Exp. Ther.* **304**, 833-840.

Weltens, R., Leyssens, A., Zhang, A. L., Lohhrmann, E., Steels, P. and van Kerkhove, E. (1992). Unmasking of the apical electrogenic H pump in isolated Malpighian tubules (*Formica polyctena*) by the use of barium. *Cell. Physiol. Biochem.* **2**, 101-116.

Weng, X. H., Huss, M., Wieczorek, H. and Beyenbach, K. W. (2003). The V-type $H(^+)$-ATPase in Malpighian tubules of *Aedes aegypti*: localization and activity. *J. Exp. Biol.* **206**, 2211-2219.

Wessing, A., Bertram, G. and Zierold, K. (1993). Effects of bafilomycin A1 and amiloride on the apical potassium and proton gradients in *Drosophila* Malpighian tubules studied by X-ray microanalysis and microelectrode measurements. *J. Comp. Physiol. B* **163**, 452-462.

Wieczorek, H., Brown, D., Grinstein, S., Ehrenfeld, J. and Harvey, W. R. (1999). Animal plasma membrane energization by proton motive V-ATPases. *BioEssays* **21**, 637-648.

Wiehart, U. I., Klein, G., Steels, P., Nicolson, S. W. and Van Kerkhove, E. (2003). K^+ transport in Malpighian tubules of *Tenebrio molitor L.*: is a K_{ATP} channel involved? *J. Exp. Biol.* **206**, 959-965.

Zhang, Z. R., Cui, G., Zeltwanger, S. and McCarty, N. A. (2004). Time-dependent interactions of glibenclamide with CFTR: kinetically complex block of macroscopic currents. *J. Membr. Biol.* **201**, 139-155.